Proc. Natl. Acad. Sci. USA
Vol. 94, pp. 9445–9450, August 1997
Neurobiology

Essential role of POU–domain factor Brn-3c in auditory and vestibular hair cell development

(inner ear development)

MENGQING XIANG*†, LIN GAN†‡, DAQING LI†§, ZHI-YONG CHEN*, LIJUAN ZHOU¶‖, BERT W. O'MALLEY, JR.§, WILLIAM KLEIN‡**, AND JEREMY NATHANS¶‖**††

*Center for Advanced Biotechnology and Medicine, Department of Pediatrics, University of Medicine and Dentistry of New Jersey–Robert Wood Johnson Medical School, Piscataway, NJ 08854; ‡Department of Biochemistry and Molecular Biology, University of Texas M.D. Anderson Cancer Center, Houston, TX 77030; Departments of §Otolaryngology, Head and Neck Surgery, ¶Molecular Biology and Genetics, ††Neuroscience and Ophthalmology, ‖Howard Hughes Medical Institute, Johns Hopkins University School of Medicine, Baltimore, MD 21205

Contributed by Jeremy Nathans, June 11, 1997

ABSTRACT **The *Brn-3* subfamily of POU–domain transcription factor genes consists of three highly homologous members—Brn-3a, Brn-3b, and Brn-3c—that are expressed in sensory neurons and in a small number of brainstem nuclei. This paper describes the role of *Brn-3c* in auditory and vestibular system development. In the inner ear, the Brn-3c protein is found only in auditory and vestibular hair cells, and the Brn-3a and Brn-3b proteins are found only in subsets of spiral and vestibular ganglion neurons. Mice carrying a targeted deletion of the *Brn-3c* gene are deaf and have impaired balance. These defects reflect a complete loss of auditory and vestibular hair cells during the late embryonic and early postnatal period and a secondary loss of spiral and vestibular ganglion neurons. Together with earlier work demonstrating a loss of trigeminal ganglion neurons and retinal ganglion cells in mice carrying targeted disruptions in the *Brn-3a* and *Brn-3b* genes, respectively, the *Brn-3c* phenotype reported here demonstrates that each of the *Brn-3* genes plays distinctive roles in the somatosensory, visual, and auditory/vestibular systems.**

A number of transcription factors have been implicated in decisions related to neuronal vs. nonneuronal cell fate, regional specification in the nervous system, or determination of the terminally differentiated phenotype. For example, bHLH factors such as neuroD and the achaete–scute family control neural vs. ectodermal cell fates (1, 2), Hox genes control regional specification along the neuraxis (3), and several POU–domain genes act at late stages to control the survival and final differentiated phenotype of particular neuronal subtypes (4). The POU–domain family was intially defined by the mammalian pituitary-specific transcription factor Pit-1/GHF-1, the octamer binding proteins Oct-1 and Oct-2, and the *Caenorhabditis elegans* gene *Unc-86* (5). Genetic studies in mice and humans indicate that many POU–domain genes function in the terminal stages of central nervous system development. *SCIP/Tst-1/Oct-6* controls the differentiation of Schwann cells (6–8), *Pit-1/GHF-1* is required for the normal development of the anterior pituitary (9), *Brn-4/RHS2/POU3F4* is required for the normal development of the middle ear (10), and *Brn-2* is required for the specification of subsets of neurons in the hypothalamus (11, 12).

The class IV POU–domain group is defined by the *Unc-86* gene (13), the *Drosophila I-POU* gene (14, 15), and the three vertebrate *Brn-3* genes (16–20). The Unc-86 protein is found exclusively within a subset of neurons and neuroblasts, and *Unc-86* loss-of-function mutations affect some of these cells by causing a daughter cell to assume the fate of its mother or by altering cell phenotypes postmitotically (21–23). In mammals, the three highly homologous class IV POU–domain genes, *Brn-3a*, *Brn-3b*, and *Brn-3c* (also referred to as *Brn-3.0*, *Brn-3.2*, and *Brn-3.1*, respectively), are expressed in distinct but overlapping patterns in the developing and adult brainstem, retina, and dorsal root and trigeminal ganglia (16, 18–20, 24, 25).

Targeted mutations in *Brn-3a* and *Brn-3b* have revealed a high degree of functional specificity *in vivo*. Targeted deletion of the *Brn-3a* gene results in a decreased number of neurons in the trigeminal ganglia, altered gene expression in the dorsal root and trigeminal ganglia, and defects in brainstem nuclei involved in sensory processing and motor control (26, 27). Targeted deletion of the *Brn-3b* gene results in a selective absence of ≈70% of retinal ganglion cells with little or no effect on other neurons (28, 29). In this paper we show that *Brn-3c* is expressed in auditory and vestibular hair cells and that targeted deletion of *Brn-3c* leads to defective inner ear function secondary to a complete absence of sensory hair cells. Results similar to those described here have been reported by Erkman *et al.* (29).

MATERIALS AND METHODS

Targeted Deletion of Brn-3c. To generate the gene targeting construct, the 4.8-kb *Bam*HI–*Eco*RI fragment containing the *Brn-3c* gene was cloned into the *Bam*HI site of pMCTK (L.G., unpublished work). Subsequently, the 1.8-kb *Xho*I–*Xho*I fragment containing the first exon and the majority of the second exon, and encompassing most of the coding region of *Brn-3c*, was replaced with a 1.6-kb *Xho*I–*Xho*I segment containing the PGK*neo* cassette. The targeting vector was linearized at a unique *Not*I site and 25 μg of linearized DNA was electroporated into 10^7 AB1 embryonic stem (ES) cells that were then selected for resistance to G418 and 1-(2-deoxy-2-fluoro-β-D-arabinofuranosyl)-5-iodouracil (FIAU). Among the 288 ES colonies resistant to G418 and FIAU, 7 contained the expected homologous recombination event, as indicated by Southern blot analysis using flanking probes. Two targeted ES cell clones were injected into C57BL/6J blastocysts to generate chimaeric mice, and the chimaeric mice were bred to C57BL/6J mice to produce heterozygotes and homozygotes for further analysis.

Behavioral Testing. Hearing was tested by observing the startle response. Mice were placed individually in a small

The publication costs of this article were defrayed in part by page charge payment. This article must therefore be hereby marked "*advertisement*" in accordance with 18 U.S.C. §1734 solely to indicate this fact.

Abbreviations: ES, embryonic stem; E, embryonic day; SPL, sound pressure level; DAPI, 4′,6-diamidino-2-phenylindole; P, postembryonic day.

†M.X., L.G., and D.L. contributed equally to this work and should be considered co-first authors.

**To whom reprint requests should be addressed.

Plexiglas restrainer in a sound-insulated room. At 10-sec intervals, each animal was exposed five times to a sharp sound produced by striking a metal rod. Ten *Brn-3c* (+/+), 10 *Brn-3c* (+/−), and 11 *Brn-3c* (−/−) animals were tested. Balance was tested by placing mice individually on a soft rubber-coated horizontal drum 6 cm in diameter and 5.5 cm deep, positioned 15 cm above a cushioned pad. In 1 set of 10 trials the drum was stationary, and in a second set of 10 trials the drum was rotated by a variable speed motor at 7 rpm. In each trial the mouse was observed for 60 sec after it was placed on the drum and the time elapsed until it fell from the drum was recorded. Seven *Brn-3c* (+/+), 7 *Brn-3c* (+/−), and 7 *Brn-3c* (−/−) animals were tested.

Auditory Brainstem Responses. Auditory-evoked brainstem responses were recorded using a Nicolet Compact Four (Nicolet). Mice were anesthetized with Avertin by intraperitoneal injection, and electrodes were placed at the vertex (active), bilaterally in the neighborhood of the postauricular bullae (reference), and in the forehead (ground). The acoustic stimulus consisted of a click of approximately 0.1 msec duration, presented at a rate of 11.4 per second. Responses were averaged over 1,000 stimuli. Auditory thresholds were determined by visual inspection of response traces obtained at stimulus intervals of 5 dB. Absolute stimulus intensities were calibrated to obtain the sound pressure level (SPL).

Semi-Thin Plastic Sections. Deeply anesthetized mice were perfused transcardially with PBS, 2% paraformaldehyde, 2% gluteraldehyde, 1 mM $CaCl_2$, 1 mM $MgCl_2$. Following dissection of the temporal bone, the stapes was removed from the oval window, the round window was perforated, and a small hole was made in the apex of the cochlea. The cochlea and the vestibular system were gently perfused with the same fixative, immersion fixed on ice for 2 hr, and then gently perfused with PBS, 1% osmium tetroxide. After immersion fixation in osmium tetroxide for 2 hr on ice in the dark, the temporal bones were rinsed with PBS, fixed overnight in PBS, 2% paraformaldehyde, 2% gluteraldehyde, and decalcified for 7–10 days in PBS, 0.1 M EDTA, 0.1% gluteraldehyde. Fixed and decalcified temporal bones were dehydrated and embedded in Spurr's resin (30). One micrometer sections were stained with methylene blue.

Scanning Electron Microscopy. A detailed description is presented in ref. 31.

Whole Mounts of the Organ of Corti. Temporal bones were harvested, locally perfused, and immersion fixed for 2 hr in 4% paraformaldehyde/PBS. Following dissection of the bony cochlea as described (31), the organ of Corti and immediately adjacent tissue were stained with 0.5% cresyl violet and mounted in glycerin. Acetylcholine esterase histochemistry (32) was performed in the presence of ethoxypropazine hydrochloride at 0.1 mM to inhibit pseudocholinesterase (33). Cochleas were locally perfused, dissected at the apex to reveal one turn of the organ of Corti, fixed overnight in PBS, 4% paraformaldehyde, and reacted for 4 hr at 4°C to reveal acetylcholinesterase activity.

Immunostaining. Affinity-purified rabbit anti-Brn-3a, anti-Brn-3b, and anti-Brn-3c antibodies have been described (20). Each of these antibodies specifically recognizes the Brn-3 family member against which it was raised as determined by the distinctive patterns of immunostaining obtained with each antibody and by the selective elimination of immunostaining in mice lacking the corresponding gene (refs. 20, 26, and 28; this work). For immunostaining of cochlear whole mounts, temporal bones were dissected as described above and the cochlea was locally perfused with 4% paraformaldehyde/PBS, opened at the apex to reveal one turn of the organ of Corti, fixed for 24 hr in PBS/4% paraformaldehyde, and processed for immunostaining as previously described for retina whole mounts (20). Following immunostaining, the tectorial membrane was removed, and the organ of Corti was isolated from the bony cochlea, stained with 4′,6-diamidino-2-phenylindole (DAPI), and mounted in glycerin. Immunostaining of the developing auditory and vestibular system was performed on animals after up to 5 days of postnatal development without decalcification as described (20).

RESULTS

Defective Hearing and Balance in Mice Homozygous for a Targeted Deletion of the *Brn-3c* Gene. To assess the role of *Brn-3c in vivo*, a targeted deletion of this gene was constructed in ES cells and introduced via blastocyst fusion into the mouse germ line. *Brn-3c* heterozygotes [(+/−)] are indistinguishable from the wild-type [(+/+)] in viability, fertility, and readily observable behaviors. They are also indistinguishable by all of the histologic criteria described below. *Brn-3c* homozygotes [(−/−)] have normal viability, but are 10–20% smaller than wild type, have low fertility, and spend much of their time running in circles. We think that the low weight and fertility of *Brn-3c* (−/−) mice may be secondary to the circling behavior and the resulting higher energy expenditure.

Circling behavior has been described for a number of mouse lines with inner ear defects (34). As a first step in examining inner ear function, we determined whether a sharp sound could elicit a startle response in *Brn-3c* (+/+), (+/−), and (−/−) mice. *Brn-3c* (+/+) and (+/−) mice show a robust startle response (10 mice for each genotype), whereas *Brn-3c* (−/−) mice show no response (11 mice). To begin to localize the site of the defect and to quantitatively assess audition, auditory brainstem responses were recorded from *Brn-3c* (+/+), (+/−), and (−/−) mice. Fig. 1*A* shows representative auditory brainstem responses from *Brn-3c* (+/−) and (−/−) mice. As with the wild type, *Brn-3c* (+/−) mice have an auditory threshold of approximately 50 dB SPL. In contrast, *Brn-3c* (−/−) mice show no response at any stimulus level, including 114 dB SPL, the highest level tested.

To assess vestibular function, two quantitative tests were performed. In one test, mice were placed individually on a horizontal drum, and the time elapsed until they fell from the

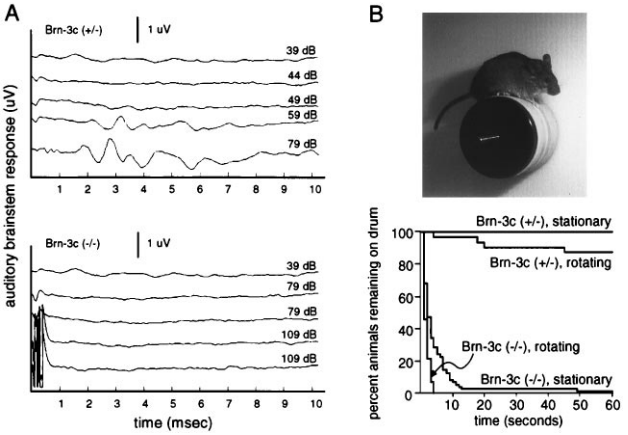

FIG. 1. Auditory brainstem responses and balancing defects in *Brn-3c* (−/−) mice. (*A*) Representative auditory brainstem responses to a click stimulus are shown at different stimulus intensities. *Brn-3c* (+/−) mice show a threshold between 49 and 59 dB SPL and robust responses at and above 59 dB SPL. *Brn-3c* (−/−) mice show no response at any stimulus level, including 109 dB SPL, the highest level shown here. The traces at 109 dB SPL show a stimulus artifact in the first 1 μsec. Traces were produced by averaging over 1,000 responses. (*B Upper*) A *Brn-3c* (+/−) mouse is shown balancing on a stationary drum. (*Lower*) Percentage of animals remaining on the drum during the 60 sec following their placement on it. Each of seven animals of the indicated genotypes was tested in 10 trials in which the drum was stationary and in 10 trials in which the drum was rotating at 7 rpm, a total of 70 trials for each genotype and test condition.

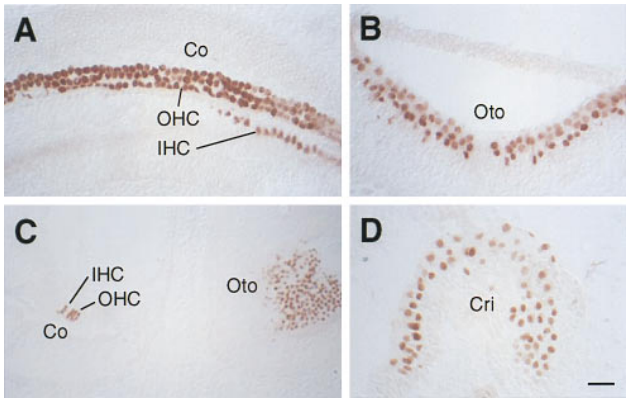

FIG. 2. Brn-3c in the developing mouse inner ear. Immunostaining with anti-Brn-3c antibodies of frozen sections at E17.5 (*A* and *B*) and E19.5 (*C* and *D*). Staining is present in the nuclei of developing hair cells at all stages shown, and is absent from other cell types. Cri, crista; Co, cochlea; Oto, otolith organ; IHC, inner hair cells; OHC, outer hair cells. [Scale bar = 50 μm (*C*) and 25 μm (*A*, *B*, and *D*).]

drum was recorded (Fig. 1*B*). *Brn-3c* (+/+) and (+/−) animals rarely fell from the drum, even when it was slowly rotated. In contrast, *Brn-3c* (−/−) mice exhibit extremely poor balance, typically falling from a stationary drum within 10 sec. When the drum was slowly rotated, forcing the *Brn-3c* (−/−) animals to walk, none remained on the drum after 5 sec. As a second test of vestibular function, we monitored the ability of mice to remain upright and swim effectively in a tub of water. Twelve *Brn-3c* (+/+) and 12 *Brn-3c* (+/−) mice remained upright and swam, whereas each of 5 Brn-3c (−/−) mice tested tumbled about when placed in the water.

Expression of Brn-3c in the Developing and Adult Inner Ear. The behavioral and electrophysiological defects described above are consistent with a primary defect in the inner ear of *Brn-3c* (−/−) mice. Therefore, as an initial step in examining the possibility that *Brn-3c* might play a role in inner ear development or function, we immunostained the developing and adult inner ear with affinity-purified anti-Brn-3c antibodies. In our earlier immunocytochemical analysis of Brn-3c, all regions of the adult central nervous system were examined except for the inner ear, leaving open the possibility that *Brn-3c* might be expressed there (20).

During late embryonic and early postnatal development, Brn-3c immunolabeling was observed specifically in developing auditory and vestibular hair cells (Fig. 2). From this analysis, it appears that all hair cells within the organ of Corti, otolith organs, and cristae express Brn-3c by embryonic day (E)15.5, the earliest time examined. As expected for a transcription factor, immunolabeling is confined to nuclei. Immunoreactivity was not observed in nonneuronal cells or in the spiral or vestibular ganglia at any developmental stage. The peak times during which auditory and vestibular hair cells undergo their final mitoses are at E14 and E14–E16, respectively (35), suggesting that Brn-3c is involved in early steps in hair cell development. In contrast, Brn-3a and Brn-3b are present in many neurons within the developing and adult spiral and vestibular ganglia, but are absent from hair cells (data not shown).

In the adult cochlea, the distribution of Brn-3c protein was determined by whole-mount immunostaining. To visualize both labeled and unlabeled cells at high resolution, the organ of Corti was dissected, counterstained with DAPI, and examined under Nomarski optics (Fig. 3). Brn-3c immunolabeling is present exclusively in the nuclei of the single row of inner hair cells and the three rows of outer hair cells; the nuclei of supporting cells are unlabeled. In the adult cristae and otolith organs, Brn-3c is also present exclusively in hair cells (data not shown).

Histological Defects in the Inner Ear in Brn-3c (−/−) Mice. In adult *Brn-3c* (+/+), (+/−), and (−/−) mice the external auditory canal, tympanic membrane, and middle ear, including the malleus, incus, and stapes, are normal in appearance. Dissection of the temporal bone revealed a normal arrangement of the semicircular canals and bony cochlea. In *Brn-3c* (−/−) mice, gentle movement of the malleus produced a corresponding movement of the footplate of the stapes, indicative of normal middle ear conduction. To determine if loss of *Brn-3c* altered the number or arrangement of auditory hair cells, the apical surface of the organ of Corti was exposed by removing the tectorial membrane and examined by scanning electron microscopy (Fig. 4). In *Brn-3c* (+/+) and (+/−) mice, the organ of Corti shows an identical arrangement of inner and outer hair cell ciliary bundles, which are flanked by the microvillus-bearing apical surfaces of supporting cells. However, in *Brn-3c* (−/−) mice the apical surface of the organ of Corti was completely devoid of ciliary bundles, consisting instead of a contiguous sheet of what appears to be supporting cells.

The absence of ciliary bundles in the *Brn-3c* (−/−) organ of Corti appears to reflect an absence of inner and outer hair cells as determined by staining whole mounts of the organ of Corti with cresyl violet (Fig. 5). In the *Brn-3c* (+/+) and (+/−)

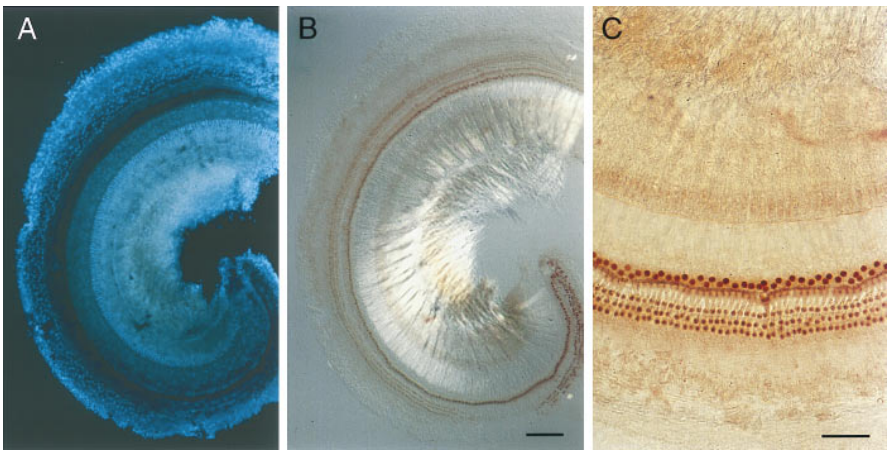

FIG. 3. Brn-3c in the adult organ of Corti. One turn of a wild-type organ of Corti adjacent to the apex is shown. The cochlea was immunostained with affinity-purified anti-Brn-3c antibodies and the dissected organ of Corti was then incubated with DAPI. (*A*) DAPI staining reveals nuclei of supporting cells that are not immunostained. (*B* and *C*) Anti-Brn3c immunoreactivity is found exclusively within the single row of inner hair cell nuclei and the three rows of outer hair cell nuclei. All hair cell nuclei are immunostained. Note that the precipitate formed by reaction of 3-amino-9-ethylcarbozole, the immunoperoxidase substrate, quenches DAPI fluorescence. [Scale bar = 100 μm (*A* and *B*) and 50 μm (*C*).]

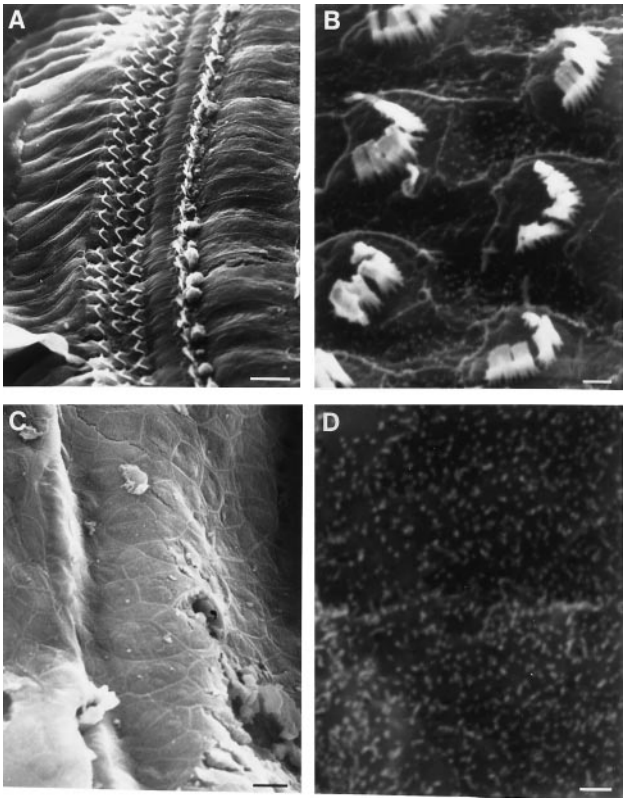

FIG. 4. Scanning electron microscopy of the organ of Corti in *Brn-3c* (+/−) and (−/−) mice. (*A* and *B*) The apical surface of the organ of Corti in *Brn-3c* (+/−) mice shows the wild-type pattern of stereociliary bundles. (*A*) Stereociliary bundles emanating from the three rows of outer hair cells are seen to the left of the stereociliary bundles emanating from a single row of inner hair cells. The four rows of hair cells are flanked by supporting cells. (*B*) A different region of the organ of Corti at high magnification shows stereociliary bundles from two rows of outer hair cells protruding above the microvilli that cover the apical face of the supporting cells. (*C* and *D*) The apical surface of the organ of Corti in *Brn-3c* (−/−) mice lacks stereociliary bundles. (*D*) At high magnification the apical surface is seen to be composed of cells bearing microvilli. [Scale bars = 10 μm (*A* and *C*) and 1 μm (*B* and *D*).]

organ of Corti there is a single row of inner hair cell bodies and three rows of outer hair cell bodies, whereas the *Brn-3c* (−/−) organ of Corti contains only sparsely located cell bodies, presumably corresponding to the supporting cells of Hensen (Fig. 5 *A* and *C*). To identify outer hair cells more specifically, efferent cholinergic synapses were visualized histochemically. In the mouse, as in other mammals, outer hair cells receive massive cholinergic innervation, which is readily visualized histochemically (32, 33). As seen in Fig. 5 *B* and *D*, in the *Brn-3c* (+/−) organ of Corti, acetylcholine esterase activity is localized to outer hair cells and to efferent nerve fibers emanating from the spiral ganglion, whereas in the *Brn-3c* (−/−) organ of Corti acetylcholine esterase activity is undetectable.

The absence of auditory hair cells in *Brn-3c* (−/−) mice could represent an isolated defect or could reflect a more general disorganization of cochlear structure. To examine this question, the cochlea was analyzed using semi-thin sections stained with methylene blue (Fig. 6). The cochleas of *Brn-3c* (−/−) mice show no aberrations in overall architecture or in the structure of Reissner's membrane or the stria vascularis, but differ from their wild-type counterparts in the absence of hair cells and the specialized architectural features immediately adjacent to hair cells. Pillar cells, which normally define the tunnel of Corti and the space of Nuel, are absent or

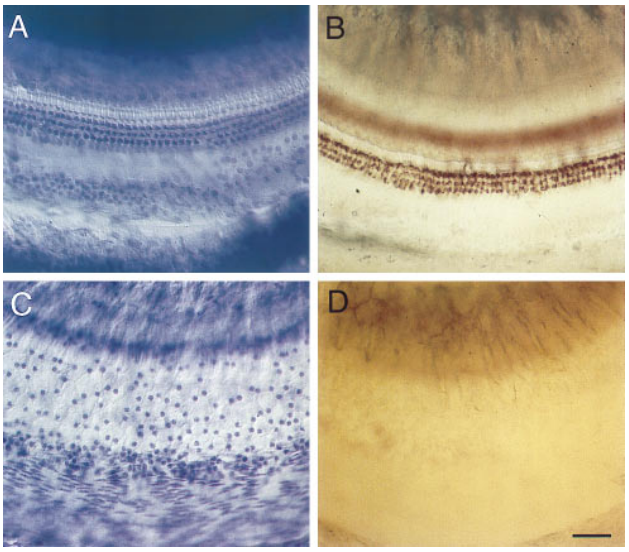

FIG. 5. Whole-mount preparation of the organ of Corti in *Brn-3c* (+/+), (+/−), and (−/−) mice. (*A*) Organ of Corti from a *Brn-3c* (+/−) mouse stained with cresyl violet shows the wild-type arrangement of a single row of inner hair cells (out of the focal plan) and three rows of outer hair cells (in the focal plane). (*B*) Organ of Corti from a *Brn-3c* (+/+) mouse stained histochemically for acetylcholine esterase reveals efferent synapses on the three rows of outer hair cells. By contrast, the organ of Corti from a *Brn-3c* (−/−) mouse lacks identifiable hair cells (*C*) and cholinergic innervation (*D*). (Scale bar = 50 μm.)

rudimentary, and cells that resemble Deiter's cells are variably present. A typical section, such as the one shown in Fig. 6*C*, reveals only a single cell type, presumably the cells of Hensen, above the basilar membrane. A second difference in the *Brn-3c* (−/−) cochlea is seen in a large reduction in the number of neurons and myelinated fibers in the spiral ganglion (Fig. 6 *B* and *D*). Because *Brn-3c* is not expressed in supporting cells or

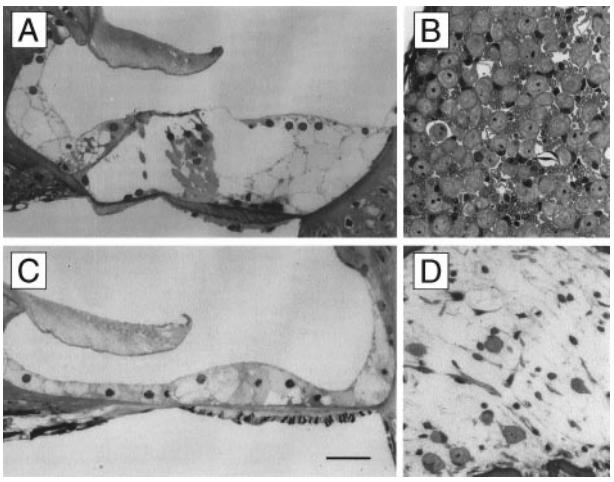

FIG. 6. Absence of hair cells in the organ of Corti and defects in the spiral ganglion in *Brn3c* (−/−) mice. (*A*) Organ of Corti from a *Brn-3c* (+/−) mouse. The single inner hair cell, the three outer hair cells, and the three underlying Deiter's cells are clearly visible. (*B*) Part of a spiral ganglion from a *Brn-3c* (+/−) mouse showing a dense packing of myelinated axons and neuronal cell bodies. (*C*) Organ of Corti from a *Brn-3c* (−/−) mouse. Inner and outer hair cells are missing and the epithelium beneath the tectorial membrane contains only supporting cells. (*D*) The spiral ganglion from a *Brn-3c* (−/−) mouse contains fewer than one-tenth as many myelinated axons and neuronal cell bodies than the spiral ganglia of *Brn-3c* (+/+) or (+/−) mice. Tissues were embedded in Spurr's resin and 1 μm sections were stained with methylene blue. (Scale bar = 25 μm.)

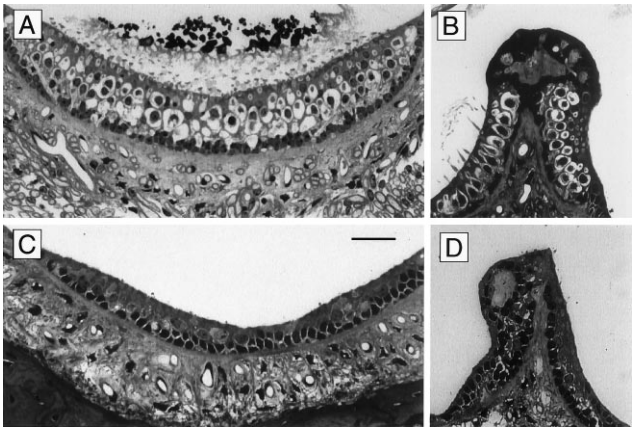

FIG. 7. Absence of hair cells in the otolith organs and cristae of *Brn-3c* (−/−) mice. (*A*) An otolith organ from a *Brn-3c* (+/−) mouse. Type I hair cells, the most abundant hair cell class, have a lightly stained nerve chalice surrounding a darkly stained cell body. Ciliary bundles can be seen protruding into the densely stained otoliths at the top. A single layer of supporting cells lies beneath the layer of hair cells. (*B*) Crista from a *Brn-3c* (+/+) mouse. Type I hair cells are abundant and their ciliary bundles are seen at the left side of the ampullary crest, where the section is nearly perpendicular to the apical surface. (*C* and *D*) Otolith organ (*C*) and crista (*D*) from a *Brn-3c* (−/−) mouse are devoid of hair cells. Presumptive supporting cells are seen within the epithelium. The density of axon bundles beneath the otolith organ is greatly reduced in the *Brn-3c* (−/−) animal. Tissues were embedded in Spurr's resin and 1 μm sections were stained with methylene blue. (Scale bar = 25 μm.)

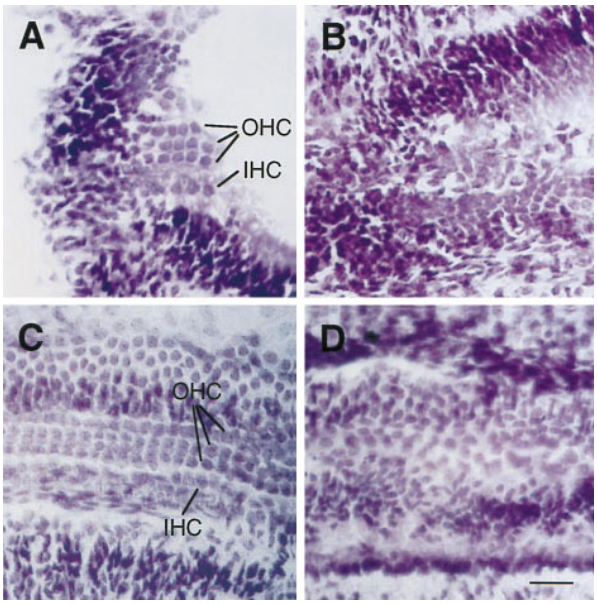

FIG. 8. Defects during development of the cochlea of *Brn-3c* (−/−) mice. Cresyl violet-stained frozen sections showing the progressive development of the organ of Corti at P1 (*A* and *B*) and P5 (*C* and *D*). (*A* and *C*) *Brn-3c* (+/−). (*B* and *D*) *Brn-3c* (−/−). The organized layering of inner and outer hair cells fails to appear in *Brn-3c* (−/−) animals. HC, hair cells; IHC, inner hair cells; OHC, outer hair cells. (Scale bar = 25 μm.)

in the spiral ganglion during development (see above), loss of supporting cells and spiral ganglion neurons is likely to be secondary to the loss of hair cells.

A similar pattern of cell loss in *Brn-3c* (−/−) mice was observed in the vestibular organs and in the vestibular ganglion. *Brn-3c* (+/+) and (+/−) vestibular organs contain a high density of type 1 hair cells in which a lightly stained nerve chalice surrounds a darkly stained cell body (Fig. 7 *A* and *B*). Numerous stereocilia protrude from the apical surface and a single layer of darkly stained supporting cells lies beneath the sensory hair cells. In *Brn-3c* (−/−) mice, the bony structure of the vestibular system and the nonsensory epithelium within it appears to be unaffected, but the sensory epithelium contains only supporting cells (Fig. 7 *C* and *D*). Few or no myelinated axons are seen beneath the otolith organs in *Brn-3c* (−/−) mice.

The absence of auditory and vestibular hair cells in adult *Brn-3c* (−/−) mice could reflect a failure of these cells to develop or survive at any stage prior to adulthood. To identify the time during development when hair cell loss occurs, inner ears of *Brn-3c* (+/+), (+/−), and (−/−) animals were examined at E17.5, E19.5, postembryonic day (P)1, and P5 by cresyl violet staining and by immunostaining with antibodies directed against Brn-3a and Brn-3b. This analysis revealed a progressive disorganization and loss of both auditory and vestibular hair cells as early as E17.5 with nearly complete loss by P5 (Fig. 8), suggesting that Brn-3c may not be required for the initial production of hair cells, but is required for their correct development and survival. Neuronal loss within the spiral and vestibular ganglia occurs later, with minimal cell loss at E17.5, clearly reduced numbers of neurons at P1 and P5, and severe depletion of neurons and myelinated fibers by several months of age (data not shown). *Brn-3c* is also expressed in approximately 30% of retinal ganglion cells, in a minority of neurons in the dorsal root and trigeminal ganglia, and in scattered cells within several nuclei in the midbrain (20). By cresyl violet staining we did not observe any differences in the size, number, or arrangement of neurons in the retina, dorsal root and trigeminal ganglia, and midbrain in *Brn-3c* (+/+), (+/−), or (−/−) mice at E17.5, E19.5, P1, and P5.

DISCUSSION

This paper describes the consequences of targeted deletion of the POU–domain transcription factor *Brn-3c*. *Brn-3c* (−/−) mice exhibit severe defects in balance and hearing and they show a rapid and progressive loss of auditory and vestibular hair cells during late gestation and early postnatal life. Spiral and vestibular ganglion neurons degenerate over the ensuing weeks, but the middle ear and the overall architecture of the inner ear are unaffected. This phenotype is consistent with the observed pattern of Brn-3c immunoreactivity. In the inner ear, Brn-3c is found exclusively in auditory and vestibular hair cells beginning at least as early as E15.5. The degeneration of the spiral and vestibular ganglia in *Brn-3c* (−/−) mice is consistent with the previously described expression of brain-derived neurotrophic factor and neurotrophin-3 in auditory and vestibular hair cells (36–39) and the essential role of these neurotrophic factors in the survival of spiral and vestibular ganglion neurons (40–42).

The *Brn-3c* mutant phenotype in mice may be relevant to the study of some forms of human deafness. In humans, inherited congenital or early childhood deafness affects 1 person in 2,000 (43). In approximately 30% of the cases, inherited deafness is associated with other abnormalities (syndromic deafness). The remaining 70% of the cases are unaccompanied by other abnormalities (nonsyndromic deafness), and among this group approximately 85% are caused by mutations in any of a large number of autosomal recessive genes. The *Brn-3c* (−/−) phenotype in mice suggests the human *Brn-3c* gene as a candidate gene for autosomal recessive nonsyndromic deafness, and suggests that *Brn-3c* (−/−) mice may be useful as an animal model for some forms of inherited human deafness.

The highly specific pattern of neuronal loss in *Brn-3c* (−/−) mice is reminiscent of the specific loss of most retinal ganglion cells in *Brn-3b* (−/−) mice (28, 29) and of subsets of primary somatosensory neurons in the trigeminal ganglia and selected

neurons in sensory and motor nuclei in the brainstem in *Brn-3a* (−/−) mice (26, 27). A striking feature of the three *Brn-3* mutant phenotypes is the division of defects among the somatosensory, visual, and auditory/vestibular systems. In each of these three sensory systems, the most obvious cellular phenotype, neuronal loss, is only produced by deletion of one of the *Brn-3* genes. Given the high degree of homology between the *Brn-3* genes and the likelihood that they arose from a common ancestral *Unc-86*-like gene, it is tempting to speculate that the *Brn-3* genes may act by a similar mechanism to promote cell survival. For example, neuronal loss in each of the *Brn-3* mutants might be explained if the *Brn-3* family controlled the expression of genes mediating the receipt of cell survival signals. This general possibility is suggested by the observations of McEvilly *et al.* (27) that transcripts derived from TrkB, TrkC, and the low-affinity nerve growth factor receptor (p75), are reduced in the E12.5 trigeminal ganglia of *Brn-3a* (−/−) mice, possibly presaging the loss of sensory neurons in these mice.

Thus far, descriptions of *Brn-3* knockout mice—including the present one—have not extensively explored phenotypes other than cell loss. The possibility that additional, and more subtle, phenotypes remain to be identified in these mice is suggested by the variety of effects on neuronal lineage and identity produced by *Unc-86* mutants in *C. elegans* (21–23). In vertebrates, an additional level of complexity arises from the partially overlapping patterns of expression of the *Brn-3* genes, suggesting that in some cells these genes may act in a combinatorial and/or partially redundant fashion. In this case, the earlier finding of Brn-3c in subsets of retinal ganglion cells and primary somatosensory neurons suggests that, in addition to its essential role in hair cell development and survival, Brn-3c may play a more subtle role in the development of these other neurons.

We thank J. Li and M. Delannoy for assistance with tissue sectioning and electron microscopy and P. Bhanot for helpful comments on the manuscript. This work was supported by the National Eye Institute and the National Institute of Child Health and Human Development (National Institutes of Health), the Robert A. Welch Foundation, the Retina Foundation, and the Howard Hughes Medical Institute.

1. Jan, Y. N. & Jan, L. (1993) *Cell* **75,** 827–830.
2. Lee, J. E., Hollenberg, S. M., Snider, L., Turner, D. L., Lipnick, N. & Weintraub, H. (1995) *Science* **268,** 836–844.
3. Keynes, R. & Krumlauf, R. (1994) *Annu. Rev. Neurosci.* **17,** 109–132.
4. Ryan, A. K. & Rosenfeld, M. G. (1997) *Genes Dev.* **11,** 1207–1225.
5. Herr, W., Sturm, R. A., Clerc, R. G., Corcoran, L. M., Baltimore, D., Sharp, P. A., Ingraham, H. A., Rosenfeld, M. G., Finney, M., Ruvkin, G. & Horvitz, H. R. (1988) *Genes Dev.* **2,** 1513–1516.
6. Weinstein, D. E., Burrola, P. G. & Lemke, G. (1995) *Mol. Cell. Neurosci.* **6,** 212–229.
7. Bermingham, J. R., Scherer, S. S., O'Connell, S., Arroyo, E., Kalla, K. A., Powell, F. L. & Rosenfeld, M. G. (1996) *Genes Dev.* **10,** 1751–1762.
8. Jaegle, M., Mandemakers, W., Broos, L., Zwart, R., Karis, A., Visser, P., Grosveld, F. & Meijer, D. (1996) *Science* **273,** 507–510.
9. Li, S., Crenshaw, E. B., Rawson, E. J., Simmons, D. M., Swanson, L. W. & Rosenfeld, M. G. (1990) *Nature (London)* **347,** 528–533.
10. de Kok, Y. J. M., van der Maarel, S. M., Bitner-Glindzicz, M., Huber, I., Monaco, A., Malsolm, S., Pembrey, M. E., Ropers, H.-H. & Cremers, F. P. M. (1995) *Science* **267,** 685–688.
11. Schonemann, M. D., Ryan, A. K., McEvilly, R. J., O'Connell, S. M., Arias, C. A., Kalla, K. A., Li, P., Sawchenko, P. E. & Rosenfeld, M. G. (1995) *Genes Dev.* **9,** 3122–3135.
12. Nakai, S., Kawano, H., Yudate, T., Nishi, M., Kuno, J., Nagata, A., Jishage, K., Hamada, H., Fujii, H., Kawamura, K., Shiba, K. & Noda, T. (1995) *Genes Dev.* **9,** 3109–3121.
13. Finney, M., Ruvkin, G. & Horvitz, H. R. (1988) *Cell* **56,** 757–769.
14. Treacy, M., He, X. & Rosenfeld, M. G. (1991) *Nature (London)* **350,** 577–584.
15. Turner, E. E. (1996) *Proc. Natl. Acad. Sci. USA* **93,** 15097–15101.
16. Xiang, M., Zhou, L., Peng, Y.-W., Eddy, R. L., Shows, T. B. & Nathans, J. (1993) *Neuron* **11,** 689–701.
17. Theil, T., McLean-Hunter, S., Zornig, M. & Moroy, T. (1993) *Nucleic Acids Res.* **21,** 5921–5929.
18. Gerrero, M. R., McEvilly, R., Turner, E., Lin, C. R., O'Connell, S., Jenne, K. J., Hobbs, M. V. & Rosenfeld, M. G. (1993) *Proc. Natl. Acad. Sci. USA* **90,** 10841–10845.
19. Turner, E. E., Jenne, K. J. & Rosenfeld, M. G. (1994) *Neuron* **12,** 205–218.
20. Xiang, M., Zhou, L., Macke, J., Yoshioka, T., Hendry, S. H. C., Eddy, R. L., Shows, T. B. & Nathans, J. (1995) *J. Neurosci.* **15,** 4762–4785.
21. Chalfie, M., Horvitz, H. R. & Sulston, J. E. (1981) *Cell* **24,** 59–69.
22. Desai, C., Garriga, G., McIntyre, S. L. & Horvitz, H. R. (1988) *Nature (London)* **336,** 638–646.
23. Finney, M. & Ruvkin, G. (1990) *Cell* **63,** 895–905.
24. Ninkina, N. N., Stevens, G. E. M., Wood, J. N. & Richardson, W. D. (1993) *Nucleic Acids Res.* **21,** 3175–3182.
25. Fedtsova, N. G. & Turner, E. E. (1995) *Mech. Dev.* **53,** 291–304.
26. Xiang, M., Gan, L., Zhou, L., Klein, W. H. & Nathans, J. (1996) *Proc. Natl. Acad. Sci. USA* **93,** 11950–11955.
27. McEvilly, R. J., Erkman, L., Luo, L., Sawchenko, P. E., Ryan, A. F. & Rosenfeld, M. G. (1996) *Nature (London)* **384,** 574–577.
28. Gan, L., Xiang, M., Zhou, L., Wagner, D. S., Klein, W. H. & Nathans, J. (1996) *Proc. Natl. Acad. Sci. USA* **93,** 3920–3925.
29. Erkman, L., McEvilly, R. J., Luo, L., Ryan, A. K., Hooshmand, F., O'Connell, S. M., Keithley, E. M., Rapaport, D. H., Ryan, A. F. & Rosenfeld, M. G. (1996) *Nature (London)* **381,** 603–606.
30. Spurr, A. R. (1969) *J. Ultrastruct. Res.* **26,** 31–43.
31. O'Malley, W., Li, D. & Turner, D. S. (1995) *Hearing Res.* **88,** 181–189.
32. Karnovsky, M. J. & Root, L. (1964) *J. Histochem. Cytochem.* **12,** 219–221.
33. Sobkowicz, H. M. & Emmerling, M. R. (1989) *J. Neurocytol.* **18,** 209–224.
34. Fuller, J. L. & Wimer, R. E. (1966) in *Biology of the Laboratory Mouse*, ed. Green, E. L. (McGraw–Hill, New York), pp. 609–628.
35. Ruben, R. J. (1967) *Acta Otolaryngol.* **220,** Suppl., 5–44.
36. Ernfors, P., Merlio, J.-P. & Persson, H. (1992) *Eur. J. Neurosci.* **4,** 1140–1158.
37. Pirvola, U., Ylikoski, J., Palgi, J., Lehtonen, E., Arumae, U. & Saarma, M. (1992) *Proc. Natl. Acad. Sci. USA* **89,** 9915–9919.
38. Ylikoski, J., Pirvola, U., Moshnyakov, M., Palgi, J., Arumae, U. & Saarma, M. (1993) *Hear. Res.* **65,** 69–78.
39. Schecterson, L. C. & Bothwell, M. (1994) *Hear. Res.* **73,** 92–100.
40. Avila, M., Varela-Nieto, I., Romero, G., Mato, J. M., Giraldez, F., Van de Water, T. & Represa, J. (1993) *Dev. Biol.* **159,** 266–275.
41. Pirvola, U., Arumae, U., Moshnyakov, M., Palgi, J., Saarma, M. & Ylikoski, J. (1994) *Hear. Res.* **75,** 131–144.
42. Ernfors, P., Van de Water, T., Loring, J. & Jaenisch, R. (1995) *Neuron* **14,** 1153–1164.
43. Petit, C. (1996) *Nat. Genet.* **14,** 385–391.